Resonant Raman Scattering by Raman-Active Infrared-Inactive Phonons in II-IV Semiconductors*

E. Anastassakis and C. H. Perry
Department of Physics, Northeastern University, Boston, Massachusetts 02115
(Received 14 April 1971)

The compounds in the family Mg_2X (X = Si, Ge, Sn, Pb) crystallize in the antifluorite structure and constitute small-gap semiconductors. We use Raman scattering techniques to investigate the surface light scattering of these materials. The frequencies of their long-wavelength optical phonons at 300 and 77 °K are established. From these values we were able to determine the effective force constants of the modes and compare them with values found in the literature. Second-order scattering has also been examined. The most striking feature of these materials, in connection with the present work, is the resonant scattering that they all exhibit for excitation frequencies between 2.40 and 2.71 eV. The resonance is attributed to interband electronic transitions. Good agreement is found between the present experimental results and an existing theoretical model on resonant Raman scattering.

I. INTRODUCTION

The four materials of the family Mg_2X (X = Si, Ge, Sn, Pb)[1] constitute small-bandgap semiconductors with indirect gaps of 0.6,[2] 0.6,[2,3] 0.3,[4] and 0.1 eV,[5] respectively. There is still some ambiguity about Mg_2Pb as to whether it is semiconductor or semimetal.[6] From the structural point of view, these materials crystallize according to the O_h crystal class with three independent interpenetrating fcc Bravais sublattices located at 0, $\frac{1}{4}$, and $\frac{3}{4}$ of the body diagonal 111 of the unit cell. This, known as the antifluorite (CaF_2) structure, is shown schematically in Fig. 1.

With three atoms per unit cell, group theory allows six optical branches in the vibrational dispersion curves, which degenerate into two triply degenerate points at the center of the Brillouin zone. The symmetries of these two points are described by the F_{2g} and F_{1u} irreducible representations of the O_h point group and correspond to the $\vec{q} \simeq 0$ Raman-active and infrared-active phonons, respectively. Because of the complementary principle, the F_{2g} and F_{1u} modes are infrared-inactive and Raman-inactive, respectively, in first order. The relative atomic motion for the two phonons is shown in Fig. 1. Furthermore, because of the macroscopic electric field associated with the F_{1u} mode, there is a TO-LO splitting at $\vec{q} \simeq 0$ for this phonon, with the corresponding frequencies ω_T, ω_L related through the well-known Lyddane-Sachs-Teller (LST) relation $(\omega_L/\omega_T)^2 = \epsilon_0/\epsilon_\infty$, where ϵ_0 and ϵ_∞ are the low- and the high-frequency dielectric constants for the material, respectively. The frequencies ω_L and ω_T can in principle be determined through infrared (IR) measurements, and have indeed been established for some of these materials, with varying accuracy depending on material and experimental and analytical procedure.[7,8] These frequencies (ω_L, ω_T) cannot be established through Raman scattering experiments, unless the parity restrictions, which forbid Raman scattering by the F_{1u} mode, are somehow relaxed. Intense Raman scattering by the normally Raman-inactive $\vec{q} \simeq 0$ LO phonons of all four materials may, and indeed, has been observed close to resonance, in first and second order.[9] Neutron scattering and independent theoretical calculations also represent sources of information on the values of these frequencies, as will be discussed later.

We have investigated the Raman spectra of these materials at room and liquid-nitrogen temperature, and established the frequencies of their Raman-active $\vec{q} \simeq 0$ optical phonons. From these values we were able to determine the effective force constants of the modes and compare them with values found in the literature. Second-order scattering has also been examined. Furthermore, detailed results on the observed resonance-enhanced scattering intensity for the F_{2g}-type phonons of the four materials are presented. The observed resonance pattern seems to agree with the results of a model proposed by other workers.

II. EXPERIMENTAL

The measurements were taken with a Spex 1401 double monochromator, and an I. T. T. FW130 photomultiplier operating in the photocounting mode. Argon-ion laser lines between 2.40 and 2.71 eV were used at low powers to avoid excessive heating of the samples. The power of the incident beam was measured within 5% at the position of the sample, with the sample removed. An oblique incidence geometry was used with the incident and scattered beams at right angles. Such a configuration is essentially equivalent to backward scattering from the surface of the samples, as the indices of refraction at these energies are typically larger

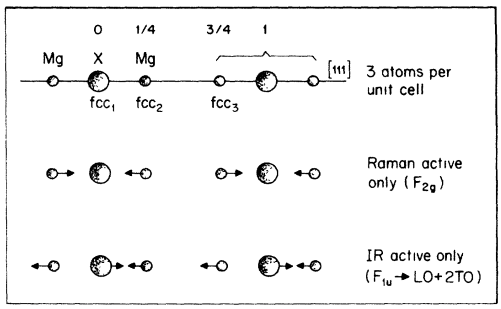

FIG. 1. Schematic presentation of the relative position and atomic displacement of the two $\vec{q} \simeq 0$ optical phonons in Mg_2X type of materials.

than five.[10] The incident beam was polarized parallel or perpendicular to the plane of incidence. The scattered light was left unpolarized. The samples used were unoriented. Cleavage surfaces corresponding to (111) planes were used for the scattering. Since these materials are particularly sensitive to moisture, the samples were kept inside an evacuated Dewar while the scattering measurements were taken. Because of the simplicity of the first-order spectrum, it was not considered necessary to make complete use of the polarization selection rules as a symmetry identification probe. Such a procedure would require oriented samples and specific polarization for the two beams, depending on their directions. Special care was taken to reproduce the same physical conditions for the scattering measurements of the four materials. This procedure allowed an approximate comparison to be made of the relative scattering intensities.

III. FIRST-ORDER RAMAN SCATTERING

The F_{2g} $\vec{q} \simeq 0$ optical phonon frequencies ω_j at 300 °K are presently established as 258.5, 255, 221, and 214 cm^{-1}, within 0.5 cm^{-1}. The relation $2\omega_j = \omega_A - \omega_S$ was used, where ω_S, ω_A are the observed absolute frequencies for the Stokes and anti-Stokes lines, respectively.[11] The observed full widths at half-intensity are 6.0 ± 0.5 cm^{-1} for X = Si, Ge, Sn and 9.5 ± 1 cm^{-1} for X = Pb, with an instrumental slit width of 1.8 cm^{-1}. These values apply to both the Stokes and anti-Stokes components. Preliminary temperature measurements on Mg_2Si gave the following results. At 77 °K the frequency increased by 3.5 cm^{-1} and the linewidth decreased by 1.5 cm^{-1}. At 420 °K the frequency decreased by 4.5 cm^{-1} and the linewidth increased by 2.5 cm^{-1}. For comparison we note that Si at 420 °K shows a decrease of frequency by 2.20 cm^{-1} and increase of the linewidth by 1.15 cm^{-1}.[12] The corresponding values for diamond and Ge are 1.7 and 0.2 cm^{-1}, and 2.4 and 0.6 cm^{-1}, respectively.[13] It appears from these figures that Mg_2Si and most likely the other materials are more anharmonic than the diamond-type covalent crystals. The values of ω_j at 77 °K are established as 262, 260, 224, and 217 cm^{-1}, within the same accuracy.

Independently of this work, two other groups of workers have reached similar values for ω_j. Buchenauer and Cardona report $\omega_j = 258.3$, 254.5, and 222.1 cm^{-1} for X = Si, Ge, Sn, respectively, at 297 °K, together with a detailed investigation of the temperature dependence of the frequency and linewidth of the mode below room temperature, using a 4880-Å 500-mW argon laser line.[14] Laughman and Davis also report $\omega_j = 258$, 220 cm^{-1} for X = Si, Sn, respectively, at room temperature, using a 4880-Å 600-mW argon laser line.[15]

It has been suggested by Buchenauer and Cardona[14] that throughout the sequence X = Si, Ge, Sn, Pb, the frequency ω_j should go as $\alpha_0^{-2.4}$, α_0 being the lattice constant. On the basis of this assumption, the values $\alpha_0 = 6.338$, 6.339, 6.762 Å for X = Si, Ge, Sn, respectively,[14] and the present value (214 cm^{-1}) of ω_j for X = Pb, we obtain the (average) value of 6.860 Å for the lattice constant α_0 of Mg_2Pb, at room temperature. This is in very good agreement with the value of 6.813 Å obtained from the literature.[14a]

IV. LATTICE DYNAMICS

Based on a model proposed by Ganesan and Srinivasan regarding expressions for the elements of the lattice vibration secular determinant of the fluorite structure,[16] Chung *et al.*[17] have reached the following expression for ω_j:

$$\omega_j^2 = (4/M)K = (4/M)(\alpha_1 + \alpha_3 + 2\beta_3) , \tag{1}$$

where M is the mass of the Mg atom, K is the effective force constant of the F_{2g} mode, and α_1 and (α_3, β_3) are force constants associated with the pairs Mg-X and Mg-Mg, respectively. These constants are related to the elastic constants C_{11}, C_{12}, C_{44} of the material as follows[16,17]:

$$\begin{aligned}
\alpha_0 C_{11} &= 2(\alpha_1 + 2\beta_2 + \alpha_3 + 3.256\, e_2^2/V) , \\
\alpha_0 C_{12} &= 2(2\beta_1 - 2\gamma_2 - \alpha_1 - \alpha_2 - \beta_2 - \beta_3 - 5.395 e_2^2/V) , \\
\alpha_0 C_{44} &= 2\left(\alpha_1 + \alpha_2 + \beta_2 + \beta_3 - 1.527 \frac{e_2^2}{V} \right. \\
&\qquad \left. - \frac{(-\beta_1 + 5.038 e_2^2/V)^2}{\alpha_1 + \alpha_3 + 2\beta_3} \right) ,
\end{aligned} \tag{2}$$

where the subscripts 1, 2, 3, on the force constants α, β, γ indicate Mg-X, X-X, and Mg-Mg neighbors, respectively. α_0 is the lattice constant, e_2 is the charge of the Mg atom and $V = \alpha_0^3/4$ is the volume of the primitive cell. Furthermore, the frequencies ω_T, ω_L of the F_{1u} mode are given by[17]

$$\omega_T^2 = (2/m + 1/M)(4\alpha_1 - \tfrac{8}{3}\pi e_2^2/V)\,,$$
$$\omega_L^2 = (2/m + 1/M)(4\alpha_1 + \tfrac{16}{3}\pi e_2^2/V)\,, \qquad (3)$$

where m is the mass of the X atom. Thus, knowledge of ω_T and ω_L from IR measurements and the LST relation can provide information on the values of α_1 and e_2 from Eq. (3).

Chung *et al.* followed the above procedure in the case of X = Si [18] and X = Ge [17] with the assumption that the short-range second-nearest-neighbor interactions are nonzero and central. It then follows that $\alpha_2 = \beta_3 = 0$ and $\beta_2 = -\gamma_2$. With this assumption and the values of α_1, e_2 obtained from Eq. (3), one can derive numerical values for the remaining constants β_1, β_2, α_3 from Eq. (2), provided the elastic constants are known. A value for ω_j can then be reached from Eq. (1).

In the case of X = Si Whitten *et al.* [18] obtained $\omega_j = 258$ cm^{-1}, using their experimental values for the elastic constants at 300 °K, which is in excellent agreement with the present results.

For X = Ge, Chung *et al.* [17] obtained $\omega_j = 262$ cm^{-1} using their experimental values for the elastic constants at 150 °K. This value (262 cm^{-1}) compares favorably with our value of $\omega_j = 260$ cm^{-1} at 77 °K within less than 1% difference. A second model considered by Chung *et al.* [17] based on the assumption that the short-range forces between Mg atoms are zero led to $\omega_j = 170$ cm^{-1}, which is by far less than the present value.

We conclude from the above two cases that the proposed point-charge model and the subsequent approximations[16-18] are fairly correct, at least in the limit of $\vec{q} \simeq 0$ and for X = Si, Ge. Later we shall see that these results for $\vec{q} \neq 0$ can also provide a reasonable interpretation for the present second-order spectra.

Davis *et al.* [19] proceeded to apply the previous point-charge model to Mg_2Sn assuming the Sn atoms to be independently (a) nonpolarizable (rigid model) and (b) polarizable (shell model). The values obtained for ω_j were 211 and 206 cm^{-1}, respectively. Since the over-all fitting of their optical dispersion curves to those recently obtained from neutron scattering by Kearney *et al.* [20] was rather poor, the latter group of workers attempted an improvement to the models of Davis *et al.* by considering a rigid-ion model, as well as nine (only Sn polarizable) and ten (both Sn and Mg polarizable) parameter versions of the shell model. A least-squares fit to the neutron scattering data with the the ten-parameter shell model gave the best over-all agreement. All three models gave the value of 222 cm^{-1} for ω_j in agreement with the neutron and Raman scattering data.

As far as Mg_2Pb is concerned, we are not aware of any theoretical or experimental source of information on its lattice dynamical properties, force constants, elastic constants, etc. Thus comparison of the presently established value $\omega_j = 214$ cm^{-1} at 300 °K is not as yet possible.

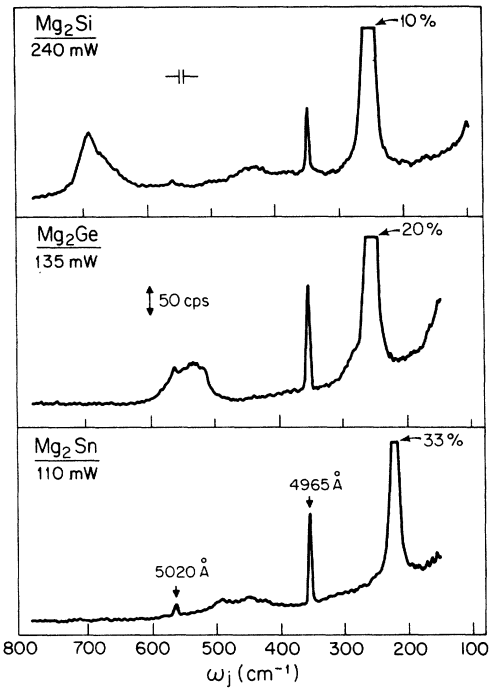

FIG. 2. Extended spectra of Mg_2Si, Mg_2Ge, and Mg_2Sn at 300 °K, using the 4880-Å excitation frequency at varying powers as indicated. When no interference filter is used, a weak laser line appears to overlap with the Stokes component of Mg_2Sn at ~225 cm^{-1}.

V. SECOND-ORDER RAMAN SPECTRA

In Fig. 2 the complete spectra for X = Si, Ge, Sn are shown taken at 300 °K with the 4880-Å argon laser line, instrumental slit width 4.7 cm^{-1}, scanning speed 10 cm^{-1}/min, and 10-sec time constant. Basically similar spectra appear in Ref. 14 without any assignments for the indicated structure. In spite of the use of a narrow-band interference filter, there is still some leakage of the 4965- and 5020-Å laser lines which are responsible for the two peaks at ~360 and 561 cm^{-1}, respectively.

Interestingly, in Mg_2Si the $\vec{q} \simeq 0$ LO phonon frequency ω_L overlaps with the 4965-Å laser line, thus prohibiting the direct observation of the LO band at ~348 cm^{-1} as established through Raman resonance measurements. [9] Its overtone $2LO_1(\Gamma)$ at ~696 cm^{-1} is clearly exhibited, broad and prominent on the top of an even broader second-order structure. [21] Furthermore, the weak peak at 560 cm^{-1} may correspond to the overtone scattering 2LA(X) according to the dispersion curves of Ref. 18 (in addition to the 5020-Å line leak). The broad band at ~430 cm^{-1} and the three weaker ones at ~500,

595, and 670 cm^{-1} are attributed to the overtone scattering $2TO_2(L)$, and $2LO_2(L)$, $2TO_1(X)$, and $2LO_1(\Sigma)$, respectively, based on the same reference. The above assignment involving overtones (without excluding combinations) is only a tentative one, inasmuch as there is so far no experimental confirmation of the complete dispersion curves of Ref. 18. No overtone $2TO_2(\Gamma) = 2LO_2(\Gamma)$ at ~ 517 cm^{-1} was observed. Instead, a strong line at 521 cm^{-1} appeared irregularly, depending on where on the sample surface was the laser focused. From anti-Stokes and temperature measurements and also from observed structure in the region 900–1050 cm^{-1}, we were able to conclude that this line was due to regular first-order Raman scattering by some kind of Si local inclusions.[12,22] At 77 °K the 258.5-, 348-, and 696-cm^{-1} lines shifted and sharpened; furthermore, there was a dramatic resonance-induced increase in their intensities.[9] Otherwise, the broad second-order bands remained practically unchanged.

The room-temperature spectrum of Mg_2Ge and Mg_2Sn shown in Fig. 2 does not appear as interesting as that of Mg_2Si. In Mg_2Ge there is some activity around 550 cm^{-1}, which according to Ref. 17 may be due to the overtone scattering $2LO(X)$ and $2LO_2(K)$ (545 and 550 cm^{-1}, respectively).

In Mg_2Sn, the second-order activity around 450 and 490 cm^{-1} may very well be attributed to overtone scattering from the zone-edge phonons X_5' and L_2', respectively, using Kearney's notation and data.[20] The same characteristic behavior as in Mg_2Si was also exhibited by both X = Ge, Sn when the temperature was lowered to 77 °K.

Finally, no second-order structure was observed at 300 or 77 °K for X = Pb, even with the highest laser power used, which, however, was rather low ($\lesssim$ 30 mW) due to the sample surface limitations under intense laser heating.

VI. RESONANT RAMAN SCATTERING BY THE F_{2g}-TYPE PHONON

The first theoretical treatment of resonant Raman scattering by optical modes in liquids and solids was given by Ovander *et al.*[23,24] and by Loudon.[25] In the recent years intense experimental effort has been put in this direction. A number of materials has been examined under resonance conditions, such as wurtzite- and zinc-blende-type semiconductors.[26–34] In all these cases the resonance was observed either at the fundamental absorption edge[26–30] or at the E_1 energy gap,[31–34] and the phonons involved were IR active and usually LO type. Birman and Ganguly[35] suggested that exciton intermediate states can be responsible for the observed resonance by LO and TO phonons. Furthermore, Burstein *et al.*[36,37] attributed the LO resonance to an exciton-phonon coupling through the Frohlich interaction, with exciton states as intermediate states; they also suggested that the TO resonance was due to processes involving continuum electron-hole pairs as intermediate states.

We were able to observe a frequency-dependent scattering intensity in the present materials Mg_2X by the F_{2g}-type phonons.

Considering the fact that this mode is IR inactive and therefore no Frohlich-interaction-type coupling can enter, and also that no intense excitonic activity is exhibited by these materials,[38] the present type of resonance cannot be approached in the same way as in the case of the TO-LO IR-active phonons.

Pinczuk and Burstein[39] have shown that in cubic materials the resonant Raman tensor due to the deformation potential of the optical phonon (j) can be written within certain approximations as

$$|R_{12}^{j}| \propto \omega_1^2 \left| \frac{\chi(\omega_1) - \chi(\omega_2)}{\omega_1 - \omega_2} \frac{dE_G}{du_j} du_j \right| , \qquad (4)$$

where $\chi(\omega_1)$ and $\chi(\omega_2)$ are the values of the complex electric susceptibility tensor at the incident and scattered frequencies ω_1 and ω_2, respectively, u_j is the optical phonon displacement, E_G is the direct energy gap, and dE_G/du_j is the deformation potential associated with the optical phonon (j). The above expression represents contributions to the Raman scattering tensor for TO and LO phonons, arising from the phonon deformation potential *only*, and includes only *two-band* scattering processes. There are five more terms in the complete expression of the Raman tensor, as originally derived by Loudon through a third-order perturbation theory,[40] but the one above exhibits the strongest enhancement under conditions of resonance. Far from resonance, these nonresonating terms should be taken into consideration as well. Finally, in deriving Eq. (4) it has been assumed that the interband momentum matrix elements and the intraband matrix elements of the electron-phonon interaction are constant for the two bands under consideration, and that $\vec{q}$-dependent terms can be neglected, i.e., Eq. (4) corresponds to the limit $\vec{q} \to 0$.

It has by now very well been established[10,41] that the present materials exhibit strong absorption activity in the range between 2 and 3 eV (the following discussion does not apply to Mg_2Pb since no experimental work on its optical properties appears to exist). According to Vazquez *et al.*,[41] the leading peak in the reflectivity spectra in the above range is considered as a possible E_1 transition ($\Lambda_3 \to \Lambda_1$ or $L_3' \to L_1$ in the usual zinc-blende notation). Secondary peaks in the same region can also be considered as due to E_2 transitions ($\Sigma_4 \to \Sigma_1$) or $K_4 \to K_1$ transitions. The energy values of these transitions are not precisely known; for instance, in Mg_2Si the E_1 transition can occur between 2.51 and 2.75 eV, depending on the origin of the experimental data

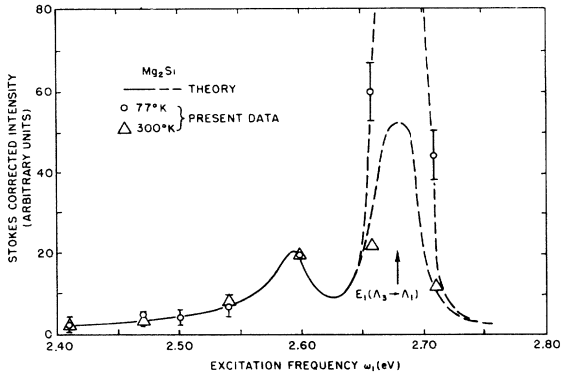

FIG. 3. Intensity pattern of the Stokes line of Mg_2Si at 77 °K. Solid line stands for the results of Eq. (5) with the values of $\epsilon(\omega)$ as taken from Ref. 10. The present experimental points at 300 and 77 °K are independently fitted to the 2.60-eV point of the theoretical curve. Laser power 28 mW.

(Table I of Ref. 41). Complete curves with the frequency dependence of the optical and dielectric properties of the three materials at 77 °K in the above range have been published by Scouler.[10] His results have been used in the following calculations in connection with the present resonant Raman scattering.

Assuming that Eq. (4) is also applicable for the present transitions, and taking dE_G/du_j as practically constant over the region of these transitions in the Brillouin zone, one finds that the frequency-normalized Raman intensity can be expressed as

$$I(\omega_2) \propto |R_{12}^j|^2 \propto [\epsilon_1(\omega_1) - \epsilon_1(\omega_2)]^2 + [\epsilon_2(\omega_1) - \epsilon_2(\omega_2)]^2 , \quad (5)$$

where $\epsilon_1(\omega)$ and $\epsilon_2(\omega)$ are the frequency-dependent real and imaginary parts, respectively, of the dielectric constant $\epsilon(\omega) = 1 + 4\pi\chi(\omega)$. Equation (5) gives the intensity of the Stokes (anti-Stokes) as the frequency ω_2 is adjusted to $\omega_S(\omega_A)$. Using Scouler's data for $\epsilon_1(\omega)$ and $\epsilon_2(\omega)$, we were able to plot the intensity pattern of the Stokes line $I(\omega_S)$ for X = Si, Ge, Sn, as shown in Figs. 3–5 in the region of resonance.

Although the position of the main resonance peaks is well established, the relative height of the peaks is ambiguous since it is very sensitive even to small changes of the constants $\epsilon_1(\omega)$ and $\epsilon_2(\omega)$. Both the experimental errors in the work of Ref. 10 as well as the subsequent Kramers-Kronig (KK) analysis may very easily introduce such small changes, which in turn affect the present intensity curves rather drastically. This situation is shown in Fig. 3 by dashed lines for two equally acceptable sets of values of $\epsilon_1(\omega)$ and $\epsilon_2(\omega)$ strictly in the region of resonance. By two equally acceptable sets of values we mean two independently taken sets of values of $\epsilon_1(\omega)$, $\epsilon_2(\omega)$ from the curves of Ref. 10, both consistent with the degree of accuracy of the results of that reference. In other words, an exact intensity pattern based on Eq. (5) is possible only when $\epsilon_1(\omega)$ and $\epsilon_2(\omega)$ are known with maximum accuracy.

The experimental data were taken using 28 mW of the following excitation lines: 2.41, 2.47, 2.50, 2.54, 2.60, 2.66, and 2.71 eV. The observed peak intensities for the Stokes components were corrected for grating efficiency, constant luminosity, photomultiplier sensitivity, the ω_1^4 law, and finally for the frequency-dependent absorption, using Loudon's formula for backward scattering,[25] i.e.,

$$I_{\text{corrected}} = (\alpha_1 + \alpha_2) I_{\text{observed}} ,$$

where $\alpha_i = 4\pi\omega_i\kappa_i$ is the absorption constant at the frequency ω_i (in cm^{-1}) and κ_i is the extinction coefficient at ω_i. Scouler's data were used for κ_i.[10] The intensity arbitrary units used in Figs. 3–5 are not related.

In Mg_2Si the resonance is established at 2.68 eV (± 0.01 eV), in agreement with the previously made comment. As shown in Fig. 3, the application of Eq. (5) results in two peaks, at ~ 2.60 and ~ 2.68 eV, with the major one attributed to the $E_1(\Lambda_3 \rightarrow \Lambda_1)$ transition.[41] The experimental data at 77 and 300 °K were taken with the incident beam polarized in the plane of incidence. The corrected experimental intensity units at the two temperatures were independently normalized to fit the theoretical value at 2.60 eV. The observed intensity increased by a factor of 4 (2) when T was decreased from 300 to 77 °K at the exciting frequency 2.66 eV (2.41 eV), i.e., close to (far from) the resonance frequency.[42]

In Fig. 4 the theoretical resonance peak for Mg_2Ge appears shifted by ~ 0.1 eV toward lower energies, relative to the observed peak which again was attributed to the E_1 $(\Lambda_3 \rightarrow \Lambda_1)$ transition.[41] It is interesting that the room-temperature data fall

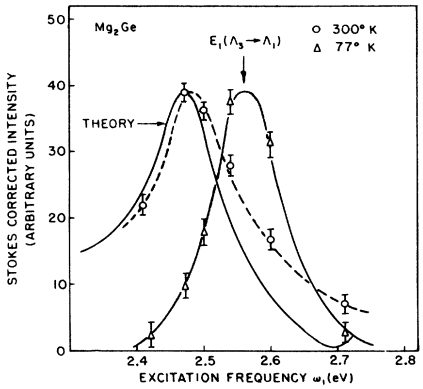

FIG. 4. Resonance intensity pattern for Mg_2Ge. The 77 and 300 °K experimental points taken with 28 mW of laser power are independently normalized to maximum intensity 40 (arbitrary units).

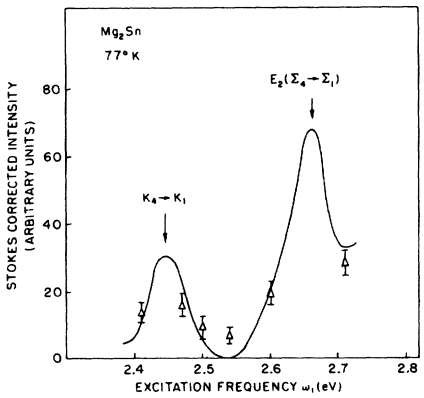

FIG. 5. Resonance intensity pattern of Mg_2Sn at 77 °K. Fitting at 2.60 eV. Laser power 28 mW.

closer to the theoretical curve which presumably corresponds to 77 °K. The normalization was made at the maximum intensity 40 (arbitrary units). Apart from the position difference of the two curves, which probably has to do with the approximations involved, the general shape and width of the two resonance curves seem to agree.

In the case of Mg_2Sn we have again two peaks, shown in Fig. 5, which according to Ref. 43 may be due to the $K_4 \rightarrow K_1$ and E_2 ($\Sigma_4 \rightarrow \Sigma_1$) transitions. With the fitting made at 2.60 eV we notice that the experimental maxima (minima) are lower (higher) than the theoretical ones. In seems reasonable to assume that such a discrepancy could be accounted for by considering the nonresonant terms which, as already discussed, were not included in Eq. (4). Such nonresonant contributions to the Raman tensor might very well interfere destructively (constructively) with the theoretical maxima (minima) of Fig. 5. At 300 °K the resonance pattern remained basically unchanged apart from an over-all decrease in intensity.

No extinction coefficient data appear to exist for Mg_2Pb. Thus, the experimental data could not be corrected for absorption. It appeared as if there was a small (less than a factor of 2) resonance increase between 2.60 and 2.71 eV. A tentatively proposed transition of $E_2(\Sigma_4 \rightarrow \Sigma_1)$ responsible for this resonance is based on recent theoretical results on the electronic band structure of Mg_2Pb published by Van Dyke and Herman.[5] According to Van Dyke,[44] $\epsilon_2(\omega)$ exhibits a very sharp peak in the region 2.40–2.70 eV. This makes the application of Eq. (5) very difficult and rather unreliable in the above region, according to the discussion following Eq. (5) of this section.

VII. SUMMARY AND DISCUSSION

First- and second-order Raman scattering measurements have been carried out for the four materials in the family Mg_2X (X = Si, Ge, Sn, Pb). At 300 °K the strength of the normal nonresonant scattering increases in the sequence X = Pb, Sn, Ge, Si with estimated peak intesities related as 1 : 2 : 4 : 5. This is only an approximate figure as the surface conditions and surface orientation were not necessarily identical for the four materials.

The present normally Raman-active (IR-inactive) F_{2g} modes exhibit intense resonance enhancement due to interband electronic transitions in the region 2.40–2.71 eV. Since the samples used in these experiments were unoriented, no investigation of polarization selection rules under conditions of resonance was attempted nor are we in position to assign any polarizations to the phonons which were responsible for the resonance. Such an assignment is straightforward in the case of polar modes, because of the LO-TO splittings. The ratio of Stokes to anti-Stokes intensities near resonance is expected to be different from its normal value of $e^{\hbar\omega_j/KT}$, according to the usual thermal population arguments. At 77 °K the bands become sharper and more intense and the resonance is further enhanced (especially in Mg_2Si where the peak becomes exceptionally strong).

A two-band model is presently used to describe the general features of resonance by the F_{2g}-type phonons.[39] This model considers only the TO- and LO-phonon deformation potential contributions to the Raman tensor in the limit $\vec{q} \rightarrow 0$ and ignores nonresonant terms. It applies to cubic materials and direct electronic transitions.

The agreement between the proposed model and our data must be considered satisfactory, especially if one takes into account the approximations involved in Eq. (4) and the arguments presented earlier regarding the numerical values of $\epsilon(\omega)$.

It is essential that the present materials offer themselves as a simple system for the study and deeper understanding of the basic principles underlying resonance in Raman scattering by nonpolar vibrational modes. Resonance-induced scattering by the normally Raman-inactive LO-type modes is another exciting aspect of the experimental possibilities of these materials. This is being independently investigated.

ACKNOWLEDGMENTS

We wish to thank Professor D. Lynch and Dr. G. A. Stringer for supplying the samples, and Dr. W. J. Scouler and Dr. J. P. Van Dyke for making their detailed optical data available to us, independently. We also acknowledge helpful discussions with Professor E. Burstein and Professor A. Pinczuk.

*Research supported in part by NASA Grant No. NGL-22-011-051 and Northeastern University, Boston, Mass. 02115.

[1]In what follows the four materials will always be taken in the same sequence, i.e., X=Si, Ge, Sn, Pb.

[2]A. Stella, A. D. Brothers, R. H. Hopkins, and D. W. Lynch, Phys. Status Solidi 23, 697 (1967).

[3]L. A. Lott and D. W. Lynch, Phys. Rev. 141, 681 (1966).

[4]H. G. Lipson and A. Kahan, Phys. Rev. 133, A800 (1964).

[5]J. P. Van Dyke and F. Herman, Phys. Rev. B 2, 1644 (1970).

[6]G. A. Stringer and R. J. Higgins, J. Appl. Phys. 41, 489 (1970) and references therein.

[7]D. McWilliams and D. W. Lynch, Phys. Rev. 130, 2248 (1963).

[8]R. Geick, W. J. Hakel, and C. H. Perry, Phys. Rev. 148, 824 (1966); also, H. G. Lipson and A. Kahan, *ibid.* 158, 756 (1967).

[9]E. Anastassakis and E. Burstein, *International Conference on Light Scattering in Solids, Paris*, 1971 (Flammarion Science, Paris, 1971); also, Solid State Commun. (to be published).

[10]W. J. Scouler, Phys. Rev. 178, 1353 (1969) and references therein.

[11]E. Anastassakis and C. H. Perry, Bull. Am. Phys. Soc. 16, 29 (1971); also, Solid State Commun. 9, 407 (1971).

[12]T. R. Hart, R. L. Aggarwal, and B. Lax, Phys. Rev. B 1, 638 (1970).

[13]E. Anastassakis, H. C. Hwang, and C. H. Perry, Phys. Rev. (to be published).

[14]C. J. Buchenauer and M. Cardona, Phys. Rev. B 3, 2504 (1971).

[14a]W. B. Pearson, *Handbook of Lattice Spacings and Structures of Metals and Alloys* (Pergamon, New York, 1967), Vol. 2, p. 310.

[15]L. Laughman and L. W. Davis, Solid State Commun. 9, 497 (1971).

[16]S. Ganesan and R. Srinivasan, Can. J. Phys. 40, 74 (1962).

[17]P. L. Chung, W. B. Whitten, and G. C. Danielson, J. Phys. Chem. Solids 26, 1753 (1965).

[18]W. B. Whitten, P. L. Chung, and G. C. Danielson, J. Phys. Chem. Solids 26, 49 (1965).

[19]L. C. Davis, W. B. Whitten, and G. C. Danielson, J. Phys. Chem. Solids 28, 439 (1967).

[20]R. J. Kearney, T. G. Worlton, and R. E. Schmunk, J. Phys. Chem. Solids 31, 1085 (1970).

[21]The indices 1 and 2 in present notation correspond to the IR- and Raman-active optical branches, respectively.

[22]J. H. Parker, D. W. Feldman, and M. Ashkin, Phys. Rev. 155, 712 (1967).

[23]L. N. Ovander, Opt. i Spektroskopiya 4, 555 (1958); Fiz. Tverd. Tela 4, 1471 (1962) [Sov. Phys. Solid State 4, 1081 (1962)].

[24]E. M. Verlan and L. N. Ovander, Fiz. Tverd. Tela 8, 2435 (1966) [Sov. Phys. Solid State 8, 1939 (1967)].

[25]R. Loudon, J. Physique 26, 677 (1965).

[26]R. C. C. Leite and S. P. S. Porto, Phys. Rev. Letters 17, 10 (1966).

[27]R. C. C. Leite, T. C. Damen, and J. F. Scott, in *Proceedings of the* 1968 *International Conference on Light Scattering Spectra of Solids*, edited by G. B. Wright (Springer-Verlag, New York, 1969), p. 359.

[28]J. F. Scott, R. C. Leite, and T. C. Damen, Phys. Rev. 188, 1285 (1969).

[29]J. F. Scott, T. C. Damen, W. T. Silfvast, R. C. C. Leite, and L. E. Cheesman, Opt. Commun. 1, 397 (1970).

[30]J. F. Scott, Phys. Rev. B 2, 1209 (1970).

[31]A. Pinczuk and E. Burstein, Phys. Rev. Letters 21, 1073 (1968); in *Proceedings of the* 1968 *International Conference on Light Scattering Spectra of Solids*, edited by G. B. Wright (Springer-Verlag, New York, 1969), p. 429.

[32]R. C. C. Leite and J. F. Scott, Phys. Rev. Letters 22, 130 (1969).

[33]A. Mooradian, Festerkorper 9, 74 (1969).

[34]D. L. Stierwalt and A. Nedoluha, Solid State Commun. 8, 309 (1970).

[35]J. L. Birman and A. K. Ganguly, Phys. Rev. Letters 17, 647 (1966); also, Phys. Rev. 162, 806 (1967).

[36]D. L. Mills and E. Burstein, Phys. Rev. 188, 1465 (1969).

[37]E. Burstein, S. Ushiuda, A. Pinczuk, and D. L. Mills, Phys. Rev. Letters 25, 814 (1970).

[38]M. Y. Au-Yang and M. L. Cohen, Solid State Commun. 6, 855 (1968).

[39]A. Pinczuk and E. Burstein, in *Proceedings of the Tenth International Conference on Physics of Semiconductors* (U. S. Atomic Energy Commission, Washington, D. C., 1970), p. 727.

[40]R. Loudon, Proc. Roy. Soc. (London) A275, 218 (1963).

[41]F. Vazquez, R. A. Forman, and M. Cardona, Phys. Rev. 176, 905 (1968).

[42]The large experimental error at 2.66 and 2.71 eV is due to the limited laser power available at those frequencies.

[43]M. Y. Au-Yang and M. L. Cohen, Phys. Rev. 178, 1358 (1969).

[44]J. P. Van Dyke (private communications).